

## Cysteines $\beta 93$ and $\beta 112$ as Probes of Conformational and Functional Events at the Human Hemoglobin Subunit Interfaces

Gregory B. Vásquez,\* Michael Karavitis,<sup>#</sup> Xinhua Ji,\* Igor Pechik,\* William S. Brinigar,<sup>§</sup> Gary L. Gilliland,\* and Clara Fronticelli<sup>#</sup>

\*Center for Advanced Research in Biotechnology of the University of Maryland Biotechnology Institute and National Institute of Standards and Technology, Rockville, Maryland 20850, <sup>#</sup>Department of Biochemistry and Molecular Biology, University of Maryland Medical School, Baltimore, Maryland 21201, and <sup>§</sup>Department of Chemistry, Temple University, Philadelphia, Pennsylvania 19122 USA

**ABSTRACT** Three variants of tetrameric human hemoglobin, with changes at the  $\alpha_1\beta_2/\alpha_2\beta_1$ -interface, at the  $\alpha_1\beta_1/\alpha_2\beta_2$ -interface, and at both interfaces, have been constructed. At  $\alpha_1\beta_2/\alpha_2\beta_1$ -interface the  $\beta 93$  cysteine was replaced by alanine ( $\beta C93A$ ), and at the  $\alpha_1\beta_1/\alpha_2\beta_2$ -interface the  $\beta 112$  cysteine was replaced by glycine ( $\beta C112G$ ). The  $\alpha_1\beta_2$  interface variant,  $\beta C93A$ , and the  $\alpha_1\beta_1/\alpha_2\beta_2$  double mutant,  $\beta(C93A+C112G)$ , were crystallized in the T-state, and the structures determined at 2.0 and 1.8 Å resolution, respectively. A comparison of the structures with that of natural hemoglobin A shows the absence of detectable changes in the tertiary folding of the protein or in the T-state quaternary assembly. At the  $\beta 112$  site, the void left by the removal of the cysteine side chain is filled by a water molecule, and the functional characteristics of  $\beta C112G$  are essentially those of human hemoglobin A. At the  $\beta 93$  site, water molecules do not replace the cysteine side chain, and the alanine substitution increases the conformational freedom of  $\beta 146\text{His}$ , weakening the important interaction of this residue with  $\beta 94\text{Asp}$ . As a result, when  $\text{Cl}^-$  is present in the solution, at a concentration 100 mM, the Bohr effect of the two mutants carrying the  $\beta 93\text{Cys} \rightarrow \text{Ala}$  substitution,  $\beta C93A$  and  $\beta(C93A+C112G)$ , is significantly modified being practically absent below pH 7.4. Based on the crystallographic data, we attribute these effects to the competition between  $\beta 94\text{Asp}$  and  $\text{Cl}^-$  in the salt link with  $\beta 146\text{His}$  in T-state hemoglobin. These results point to an interplay between the  $\beta\text{His}146$ - $\beta\text{Asp}94$  salt bridge and the  $\text{Cl}^-$  in solution regulated by the Cys present at position  $\beta 93$ , indicating yet another role of  $\beta 93$  Cys in the regulation of hemoglobin function.

### INTRODUCTION

Human erythrocyte hemoglobin functions as an oxygen carrier in the transport system that moves oxygen from the

lungs to the other tissues of the body. Each of the subunits contains a heme group that is capable of binding oxygen or other ligands. Binding of ligands is cooperative in that when oxygen binds to one of the subunits, it facilitates the binding of oxygen to the other subunits. Hemoglobin's cooperativity is associated with the allosteric transition from the T-state to the R-state (T for tense and R for relaxed) (Perutz, 1989).

The allosteric nature of hemoglobin is the result of the subunits packing in the tetramer that allows significant quaternary changes to occur during ligand binding. The tetramer assembles forming two different interfaces. The  $\alpha_1\beta_1$  (and  $\alpha_2\beta_2$ ) interface between the  $\alpha$ - and  $\beta$ -subunits of the dimer is quite stable with the relative positions of the two subunits being unmodified by the state of ligation of the protein. In contrast, two  $\alpha\beta$ -dimers assemble forming the  $\alpha_1\beta_2/\alpha_2\beta_1$ -interfaces that mediate the quaternary changes associated with ligand binding (Ackers et al., 1992).

The  $\beta$ -subunit has two cysteine residues,  $\beta 93\text{Cys}$  and  $\beta 112\text{Cys}$ , that are associated with the two hemoglobin interfaces. At the  $\alpha_1\beta_2/\alpha_1\beta_2$ -interface, a cysteine is present at position  $\beta 93$ ; this residue is highly conserved in mammalian hemoglobins. Recently, it has been proposed that  $\beta 93\text{Cys}$  plays a role in NO transport and delivery (Jia et al., 1996). The cysteine at  $\beta 112$  forms part of the  $\alpha_1\beta_1/\alpha_2\beta_2$ -interface and is not highly conserved in mammalian hemoglobins. Because these are the only cysteines present in the  $\beta$ -chains, their replacement by other residues can be used to probe conformational and functional events occurring at the two different interfaces upon ligand binding. Thus, three recom-

Received for publication 12 June 1998 and in final form 23 September 1998.

Gregory B. Vásquez and Michael Karavitis equally contributed to the paper.

Igor Pechik participated in this work at CARB as a guest scientist from the V. A. Englehardt Institute of Molecular Biology, Russian Academy of Sciences, Moscow, Russia.

Address reprint requests to Clara Fronticelli, Department of Biochemistry and Molecular Biology, University of Maryland Medical School, 108 N. Greene Street, Baltimore, MD 21201 USA. Tel: 410-706-2629; Fax: 410-706-7390; E-mail: cfrontic@umaryland.edu or Gary L. Gilliland, Center for Advanced Research in Biotechnology of the University of Maryland, Biotechnology Institute and National Institute of Standards and Technology, 9600 Gudelsky Drive, Rockville, MD 20850 USA. Tel: 301-975-2629; Fax: 301-330-3447; E-mail: gary.gilliland@nist.gov.

Xinhua Ji's present address is the National Cancer Institute-FCRDC, ABL-Basic Research Program, Box B, Frederick, MD 21702 USA.

Certain commercial equipment, instruments, and materials are identified in this paper in order to specify the experimental procedure. Such identification does not imply recommendation or endorsement by the National Institute of Standards and Technology, nor does it imply that the material or equipment identified is necessarily the best available for the purpose.

**Abbreviations used:** HbA, human hemoglobin;  $\beta C112G$ , hemoglobin variant in which  $\beta 112\text{Cys}$  has been replaced by Gly;  $\beta C93A$ , hemoglobin variant in which  $\beta\text{Cys}93$  has been replaced with Ala;  $\beta(C93A+C112G)$ , hemoglobin variant in which  $\beta\text{Cys}93$  has been replaced with Ala and  $\beta\text{Cys}112$  has been replaced with Gly; NMR, nuclear magnetic resonance.

© 1999 by the Biophysical Society

0006-3495/99/01/88/10 \$2.00

binant hemoglobins were constructed by replacement of one or both of the two cysteines.

The  $\beta 112\text{Cys}$  was replaced by glycine in order to introduce a void and thereby increase the flexibility of the  $\alpha_1\beta_1/\alpha_2\beta_2$  interface. The  $\beta 93\text{Cys}$  was replaced by alanine; this apolar substitution prevents H-bonding to  $\beta 94\text{Asp}$ , observed when  $\beta 93\text{Cys}$  was replaced with the polar serine (Luisi and Nagai, 1986), and the smaller side chain eliminates the conformational effect associated to the different exposition of the suphydryl group to the solvent observed in R- and T-state hemoglobin. The two mutations were combined in  $\beta(\text{C93A}+\text{C112G})$  in order to assess whether the combination of the two mutations would have additional effects.  $\beta\text{C112G}$  and  $\beta(\text{C93A}+\text{C112G})$  were crystallized in the deoxy form, and the structures determined at 2.0 and 1.8 Å resolution, respectively. The crystallographic analysis indicates that neither the single nor double amino acid replacement alters the tertiary folding of the protein or the T-state quaternary assembly. At the  $\beta 112$  site, the void left by the removal of the cysteine side chain is filled by a water molecule, and the functional characteristics of  $\beta\text{C112G}$  are essentially those of human hemoglobin A (HbA). At the  $\beta 93$  site, the void left by the mutation does not appear to be filled with a water molecule and the cysteine to alanine substitution increases the conformational freedom of  $\beta 146\text{His}$ , weakening the important interaction of this residue with  $\beta 94\text{Asp}$ .

Whereas the  $\beta 112\text{Cys}\rightarrow\text{Gly}$  mutation does not alter the functional characteristics of hemoglobin, the Bohr effect of the two mutants carrying the  $\beta 93\text{Cys}\rightarrow\text{Ala}$  substitution,  $\beta\text{C93A}$  and  $\beta(\text{C93A}+\text{C112G})$ , is modified when  $\text{Cl}^-$  are present in the solution. Thermodynamic analysis suggests that the  $\beta 93\text{Cys}\rightarrow\text{Ala}$  mutation hinders the contribution to the Bohr effect of a group with a  $\text{pK}_a$  lower than 7.6. Based on the crystallographic data, we attribute this phenomenon to the weakened interaction of  $\beta 146\text{His}$  and  $\beta 94\text{Asp}$ . Thus, these data suggest that  $\beta 93\text{Cys}$  plays a structural role in controlling this important interaction, pointing to yet another role of  $\beta 93\text{Cys}$  in hemoglobin function.

## MATERIALS AND METHODS

### Protein expression and purification

Growth, expression, and purification of the fusion protein followed a previously described protocol (Fronticelli et al., 1991). The extent of enzymatic cleavage was monitored by reverse-phase high performance liquid chromatography (Sanna et al., 1997). Reconstitution with the Cyano heme and the  $\alpha$ -globin was as described (Fronticelli et al., 1991). The hemoglobin was purified on an affinity column of immobilized hemoglobin (Sanna et al., 1997.) The mutant hemoglobins were constructed as previously described (Fronticelli et al., 1994). The purity of the recombinant hemoglobin was established by Paragon gel electrophoresis (Beckman, Fullerton, CA), reverse-phase chromatography, and sequencing of the first five amino acid residues. In all cases, the purity of the recombinant hemoglobin was 95% or better.

### Protein crystallization and x-ray data collection and processing

The procedures for the crystallization of  $\beta\text{C112G}$  and  $\beta(\text{C93A}+\text{C112G})$  hemoglobin variants and the x-ray data collection and processing are similar to that described by Fronticelli et al. (1994b). The crystallization procedure used was an adaptation of the procedure described by Perutz (1968). The unit cell parameters for both crystals are given in Table 1. X-ray data processing used the XENGEN program system (Howard et al., 1987). The  $\beta\text{C112G}$  (1GBV) crystal data included 50,688 total observations of 34,600 unique reflections. The redundancy of the data set is 1.46, and 92.8% of the possible reflections were observed. The unweighted  $R_{\text{sym}}$  of the data set is 0.06, and the average  $I/\sigma(I)$  at 2.0 Å resolution is 2.3. The  $\beta(\text{C93A}+\text{C112G})$  (1GBU) diffraction data set is composed of 131,074 observations of 41,926 unique reflections. This includes 82.7% of the measurable reflections at 1.8 Å resolution. The redundancy of the data is 3.1, the unweighted  $R_{\text{sym}}$  is 0.08, and the  $I/\sigma(I)$  is 1.1 in the outermost resolution shell.

### Crystal structure determination and refinement of 1GBV and 1GBU

The refinement of human, recombinant mutant hemoglobins  $\beta\text{C112G}$  and  $\beta(\text{C93A}+\text{C112G})$  used a virtually identical protocol to that of the human deoxyhemoglobin HbA (Fronticelli et al., 1994b), minimizing differences between the structures resulting from variations in experimental and/or refinement protocols. The starting model for the T-state  $\beta\text{C112G}$  and  $\beta(\text{C93A}+\text{C112G})$  structures was the high-resolution deoxyhemoglobin A structure, 2HHD (Fronticelli et al., 1994b). Initial refinement was carried out using the X-PLOR 3.1 program package (Brunger, 1992). Rigid-body refinement of the tetramer was followed by rigid-body refinement of the individual subunits to correct the position of the molecule within the unit cell. Using this procedure, the crystallographic  $R$  values [ $R = \Sigma(F_o - F_c)/\Sigma F_o$ ], summed over all hkl's (reciprocal space coordinates) dropped significantly. Next, simulated annealing was carried out with a slow cooling protocol (Brunger et al., 1990). The force fields used were based on the dictionary compiled by Engh and Huber (1991). Empirical energy parameters for the water molecules were taken from TIP3p model of the program CHARMM. The full charges of aspartate, glutamate, arginine, and lysine were turned off during both dynamics and conventional minimization. Before dynamics, the structures were minimized with 100 cycles of

**TABLE 1** Crystallographic parameters and refinement statistics for partially ligated 1GBV and deoxy-1GBU

	Partially ligated 1GBV	Deoxy 1GBU
Space group	P2 <sub>1</sub>	P2 <sub>1</sub>
Unit cell dimensions		
a (Å)	63.2	63.0
b (Å)	83.6	82.9
c (Å)	53.7	53.8
$\beta$ (°)	99.6	99.2
Resolution (Å)	6.0–2.0	6.0–1.8
$R_{\text{sym}}^1$	0.06	0.08
Reflections ( $I > 2 \sigma(I)$ )	34,600	41,926
Number of protein atoms	4556	4550
Number of solvent molecules	367	454
$R$ value	0.18	0.17
Deviations, rms:		
Bond distances (Å)	0.02	0.02
Angle distances (Å)	0.04	0.04

<sup>1</sup> $R_{\text{sym}} = G(I_{ij} - G_{ij}\langle I_j \rangle)/G|I_{ij}|$  in which  $G_{ij} = g_i + A_s s_j + B_s s_j^2$ ;  $s = \sin^2/\lambda$ ;  $g$ ,  $A$ , and  $B$  are scaling parameters.

conjugant gradient minimization to relieve bad contacts. The final crystallographic  $R$  value after annealing was 0.24 for 1GBV and 0.22 for 1GBU.

Further refinement for both structures was carried out on a CRAY Y-MP computer with GPRLSA (Furey et al., 1982), a restrained least-squares refinement procedure (Hendrickson, 1985), with periodic adjustments of the model using FRODO (Jones, 1978) or O (Jones et al., 1991). Two types of electron density maps were used in the fitting,  $2F_o - F_c$  and  $F_o - F_c$  maps. Contour levels for the  $2F_o - F_c$  and  $F_o - F_c$  map ranged from 0.70 to 1.0  $\sigma$  and 2.0 to 3.0  $\sigma$ , respectively. Multiple rounds of refinement, 30 for  $\beta$ C112G and 20 for  $\beta$ (C93A+C112G), followed by model adjustment were performed to eliminate difference peaks in the  $F_o - F_c$  map above 3.0  $\sigma$  and account for all of the  $2F_o - F_c$  electron density. A summary of the refinement statistics is presented in Table 1.

The coordinates and structure factors of the two hemoglobin variants have been deposited in the Brookhaven Protein Data Bank with entry identifiers 1GBV for  $\alpha$ -oxy- $\beta$ -deoxy- $\beta$ (C112G) and 1GBU for deoxy- $\beta$ (C93A+C112G).

## Oxygen equilibrium curves

Oxygen equilibrium measurements were performed using the thin layer dilution technique of Dolman and Gill (1978) with an AVIV 14DS spectrophotometer. Formation of methemoglobin as judged by spectral decomposition of the initial and final spectra was less than 10%, eliminating the need for adding a reducing system. Protein concentration was between 1.5 and 2.0 mM in heme, a concentration at which dimers and their associated complications are negligible. The buffer was 50 mM MES/HEPES/TAPS, depending on the pH + 100 mM  $\text{Cl}^-$ , temperature 25°C. The binding isotherms were fitted to the Adair equation (1925),

$$\frac{Y}{4} = \frac{\beta_1 P(O_2) + 2\beta_2 P(O_2)^2 + 3\beta_3 P(O_2)^3 + 4\beta_4 P(O_2)^4}{1 + \beta_1 P(O_2) + \beta_2 P(O_2)^2 + \beta_3 P(O_2)^3 + \beta_4 P(O_2)^4} \quad (1)$$

in which  $Y$  is the fractional saturation with  $O_2$ ,  $P(O_2)$  is the partial pressure of oxygen in millimeters of mercury, and  $\beta_i$  are the overall Adair constants. An iterative procedure incorporating the Marquardt algorithm was used, and the value of the median ligand activity,  $P_m$ , was determined by  $P_m = \beta_4^{-0.25}$  (Wyman and Gill, 1990). The experimental points are well described using the linkage equation

$$\log P_m = \log P_{m_0} + \log[(1 + K_1 \times X)/(1 + K_2 \times X)] \quad (2)$$

in which  $X$  represents the free protons concentration, and  $K_1$  and  $K_2$  are the proton association constants of liganded ( $K_2$ ) and unliganded ( $K_1$ ) hemoglobin. The derivative

$$\Delta H^+ = \delta \log P_m / \delta \text{pH} \quad (3)$$

yields the total number of protons exchanged with  $\delta \log P_m / \delta \text{pH}$  representing the binding capacity of the Bohr groups for the protons (Di Cera et al., 1988). Because of the inherent symmetry of Eq. 2, the maximum of the binding capacity plot corresponds on the abscissa to the median ligand activity, here indicated as  $pK_m$ , of all the Bohr effect groups, and on the ordinate to the maximum number of protons,  $\Delta H^+_{\text{max}}$ , exchanged during the R-T transition (Wyman and Gill, 1990). The area under the binding capacity curve multiplied by 2.303RT gives the total free energy of Bohr protons binding per mole of oxygen bound.

## RESULTS

### Structures of $\beta$ C112G and $\beta$ (C93A+C112G).

The structure of the  $\beta$ C112G mutant (1GBV) contains a tetramer in the asymmetric unit that consists of complete  $\alpha$ - and  $\beta$ -globin polypeptides and their associated hemes along with 367 water molecules (Table 1). Surprisingly, the

$\alpha$ -subunits of this high-salt, T-state crystalline form of hemoglobin have oxygen bound. The  $\alpha_1$ -subunit has full occupancy of the ligand, and the  $\alpha_2$ -subunit has partial occupancy (0.7). The coordinates associated with the mutation site are well determined. The region of the final  $2F_o - F_c$  electron density map in the vicinity of the mutation site is shown in Fig. 1 *a*.

The final structure of deoxy  $\beta$ (C93A+C112G) (1GBU) also contains a tetramer in the asymmetric unit and consists of complete  $\alpha$ - and  $\beta$ -globin polypeptides and their associated hemes along with 454 solvent molecules (Table 1). The mutation sites at the two interfaces again are well determined. The temperature factors of the atoms of the substituted residues in both 1GBV and 1GBU are similar to those of residues that are closely associated with the sites. The final  $2F_o - F_c$  electron density map in the vicinity of the mutation sites is shown in Fig. 1 *b* and *c*.

The best  $C_\alpha$  alignment of the mutant structures with natural deoxy HbA, 2HHD (Fronticelli et al., 1994b), shows that both deoxy  $\beta$ C112G and  $\beta$ (C93A+C112G) have similar quaternary structures to that of 2HHD, with an RMSD of 0.35 and 0.31 Å, respectively, for the full tetramers (Table 2). 1GBV and 1GBU were examined for diagnostic T- and R-state salt bridges (Perutz, 1989) and compared with 2HHD and the fully oxygenated R-state 1HHO structure (Shaanan, 1983) (Table 3). The distances measured for 1GBV are consistent with those reported for the T-state structure. The 1GBU salt bridges are also consistent with T-state structure, but there seems to be a slight perturbation caused by the  $\beta$ 93 mutation, as evidenced by an absence of the T-state, salt bridge between  $\beta_1$ Asp94 and  $\beta_1$ His146. Closer examination of this area reveals that the  $\beta_1$ His146 has rotated away from  $\beta_1$ Asp94. The  $\alpha_1$ Lys40- $\beta_2$ His146 and  $\alpha_2$ Lys40- $\beta_1$ His146 salt bridges in 1GBU are also noticeably longer than those of 2HHD or 1GBV, but are still present.

### Influence of the $\beta$ Cys112Gly and $\beta$ Cys93Ala mutations on the structure of the $\beta$ -subunits

The comparison of the  $\beta$ -subunits of 1GBV, 1GBU, and 2HHD confirms that the variant chains are nearly identical to that observed for natural hemoglobin (Figs. 2 and 3). The comparison of the structures of 2HHD (Fronticelli et al., 1994b) and both mutants in the  $\beta$ 93 and  $\beta$ 112 regions indicates nearly identical backbone and side chain conformations, location of solvent and sulfate, hydrogen bonds, and electrostatic interactions. At the  $\beta$ 112 site, the hole left by removal of the  $\beta$ -methylene and sulfhydryl when glycine replaced cysteine is filled by a single water molecule in both  $\beta$ -subunits in both mutants. This water is bound to two other water molecules that are associated with the  $\alpha$ -subunits of both mutant hemoglobins and 2HHD (Figs. 1 and 2). The electron density of the 1GBU  $\beta$ 93 sites clearly shows that cysteine has been replaced by alanine, but no solvent fills the voids left by removal of the sulfhydryl groups (Figs. 1 and 3).

Though there are no obvious perturbations at the  $\beta$ 112 mutation sites, there is a subtle change in the area of the  $\beta$ 93



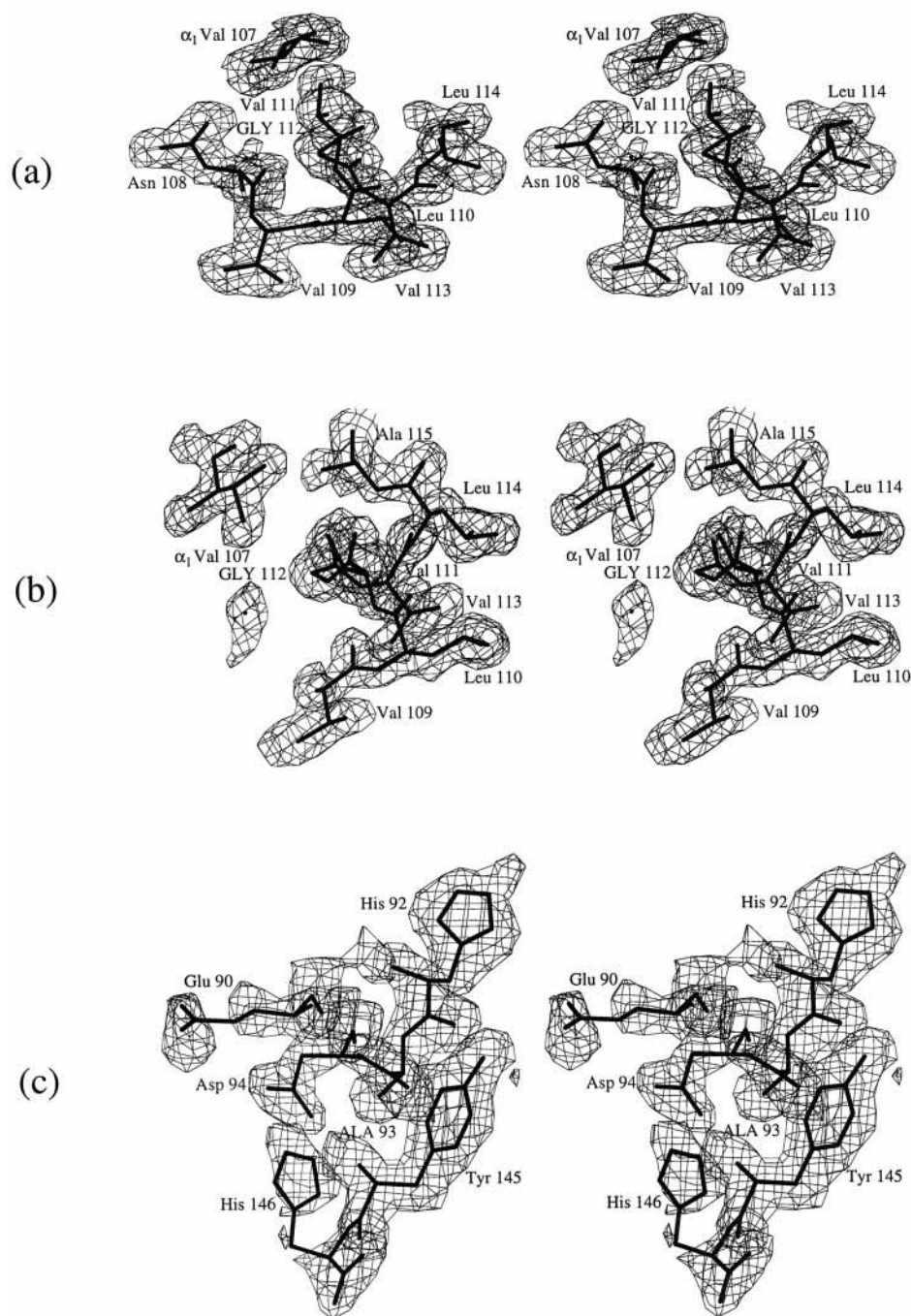


FIGURE 1 Stereoplots of the coordinates (a) of the  $\beta_1$ C112G mutation site for 1GBV, (b) of the  $\beta_1$ C112G mutation site for 1GBU, and (c) of the  $\beta_1$ C93A mutation site for 1GBU superimposed on the  $2F_o - F_c$  electron density map for each region contoured at  $1\sigma$

mutation sites. In the native deoxyhemoglobin structure, 2HHD, there is a salt bridge between  $\beta_94$  Asp and  $\beta_{146}$  His at the C-terminal residue of the same chain. In 1GBU, there is an inconsistency between the  $\beta_1$  and  $\beta_2$  subunits in which the  $\beta_2$  chain maintains the Asp94-His146 salt bridge, but the  $\beta_1$  chain does not (Fig. 3). Even in the  $\beta_2$  salt bridge that is maintained, the His146 side chain is oriented much differently than the side chains of 2HHD or 1GBV. This implies that removal of the bulky Cys93 sulfhydryl group with the change to Ala, permits His146 to sample more conformational space and adopt alternative side-chain conformations.

### Functional characteristics

In natural HbA, protons bind preferentially to the deoxygenated form of hemoglobin above pH 6.0–6.5, and this is referred to as the alkaline Bohr effect. Below pH 6.0–6.5, protons bind preferentially to the oxygenated form of hemoglobin, and this is referred to as the acid Bohr effect. The study of the pH dependence of oxygen affinity is thus a sensitive tool for investigating structure-function relationships in hemoglobin. The Bohr effect of  $\beta$ C112G was studied with oxygen equilibrium measurements, and the

**TABLE 2** Tertiary and quaternary comparisons by RMS deviations of C $\alpha$  alignments of 1GBV, 1GBU, and deoxyhemoglobin A, 2HHD

	2HHD versus		1GBV versus 1GBU (Å)
	1GBV (Å)	1GBU (Å)	
$\alpha_1$	0.27	0.25	0.21
$\beta_1$	0.24	0.24	0.19
$\alpha_2$	0.24	0.24	0.19
$\beta_2$	0.30	0.28	0.25
$\alpha_1\beta_1$	0.28	0.27	0.20
$\alpha_2\beta_2$	0.29	0.29	0.21
$\alpha_1\alpha_2\beta_1\beta_2$	0.35	0.31	0.22

binding isotherms were analyzed according to Eq. 1. Fig. 4 shows the Bohr effect of HbA and  $\beta$ C112G measured at 25°C in 50 mM MES/HEPES/TAPS + 100 mM Cl $^-$ . The points represent the experimental data, and the interpolated lines were drawn according to Eq. 2. Consistent with the absence of structural modification, as indicated by the crystallographic analysis, the Bohr effect of HbA and  $\beta$ C112G is essentially the same. In Fig. 5, the Bohr effect of  $\beta$ C112G, which is taken as the reference recombinant hemoglobin, is compared with that of  $\beta$ C93A and  $\beta$ (C93A+C112G). Whereas the oxygen affinity and the alkaline Bohr effect of the two mutants carrying the  $\beta$ 93 Cys $\rightarrow$ Ala mutation are indistinguishable, their functional characteristics are modified with respect to  $\beta$ C112G. The  $\beta$ C112G,  $\beta$ C93A, and  $\beta$ (C93A+C112G) mutants have the same oxygen affinity until  $\sim$ pH 7.5, but in the  $\beta$ 93 mutants, the Bohr effect is modified, practically ending at pH 7.4. These functional modification were, however, not observed when the Bohr effect measurements were carried out in the absence of Cl $^-$ . This is shown in Fig. 6 in which the Bohr

effect of HbA,  $\beta$ C112G, and  $\beta$ (C93A+C112G) is practically indistinguishable.

The proton binding capacity of HbA and the mutant hemoglobins was derived using Eq. 3. The related parameters are listed in Table 4. In the absence of Cl $^-$ , HbA and the three mutant hemoglobins have identical binding capacities, the  $pK_m$  of the Bohr effect groups is 7.0, the maximum number of proton released  $\Delta H_{\max}^+$  is 0.54/heme, and the free energy of proton binding is 1.4 kcal/mol. In the presence of 100 mM Cl $^-$ , HbA and  $\beta$ C112G have the same protons binding capacity; however, as indicated in Fig. 7, differences are present between  $\beta$ C112G and the  $\beta$ 93Cys $\rightarrow$ Ala mutant hemoglobins. In the  $\beta$ 93 mutants, the  $pK_m$  of the Bohr effect groups is shifted 0.4 units of pH from 7.6 to 8.0, the maximum number of protons released is decreased from 0.63 to 0.49/heme, the free energy of proton binding is decreased from 1.8 to 1.3 kcal/mol.

## DISCUSSION

### Influence of the $\beta$ 93 and $\beta$ 112 mutations on the structure of $\beta$ C112G and $\beta$ (C93A+C112G).

Perhaps not surprisingly, only small perturbations in the structure are observed in the comparison of the T-state structures of the variant hemoglobins  $\beta$ C112G and  $\beta$ (C93A+C112G) with natural T-state deoxyhemoglobin, 2HHD. Also, there is no obvious correlation between the structure and the ligation state of the single site mutant,  $\beta$ C112G, and that of the double site mutant,  $\beta$ (C93A+C112G). This is not too surprising as there is little change in the  $\alpha\beta$  dimer interface with ligand binding. The waters that fill the void left by the removal of the Cys112 side chain in its replacement by Gly appear to compensate for the lost van der Waals area and preserve the integrity of the structure in those areas of both mutant structures, 1GBV and 1GBU. The mutation at the  $\beta$ 93 site is more complicated because the Cys $\rightarrow$ Ala substitution seems to influence the conformation of the C-terminal His146. The cavity left by the mutation is not large enough to accommodate a water molecule that could maintain a van der Waals contact with His146. The 1GBU  $\beta$ His146 is then able to sample more conformational space, which may enable more dynamic movement in the T-state, and that may in turn account for the loss of the salt bridge in the  $\beta_1$  subunit and the altered positioning in the  $\beta_2$  subunit.

### Functional characteristics

Differential gel filtration measurements indicated that the mutation  $\beta$ 93Cys $\rightarrow$ Ala or  $\beta$ 112Cys $\rightarrow$ Gly does not modify the dimer-tetramer association constants (Fronticelli et al., 1994a). Thus, also in solution these recombinant hemoglobins have the tetrameric assembly of natural HbA. The absence of conformational modifications in  $\beta$ C112G is reflected in its functionality, which is similar to that of natural HbA (Fig. 4, Table 4). The replacement of the cysteine side chains with a water molecule probably prevents the mani-

**TABLE 3** Comparison of diagnostic T- and R-state salt bridge distances of 1GBV and 1GBU to deoxyhemoglobin A, 2HHD, and the fully oxygenated 1HHO structure

Salt Bridge	Distances (Å)				Diagnostic state (T/R)
	2HHD	1GBU	1GBV	1HHO	
R/T State	T	T	T	R	
$\alpha_1$ V1- $\alpha_1$ S131	4.6	5.4	6.3	4.9	T
$\alpha_2$ V1- $\alpha_2$ S131	5.9	6.0	5.8	4.9	T
$\alpha_1$ K127- $\alpha_2$ R141	2.9	2.9	2.8	20.9	T
$\alpha_1$ D126- $\alpha_2$ R141	2.8	2.6	2.5	12.4	T
$\alpha_2$ K127- $\alpha_1$ R141	3.2	2.7	3.1	20.9	T
$\alpha_2$ D126- $\alpha_1$ R141	2.7	2.6	2.6	12.4	T
$\alpha_1$ Y42- $\beta_2$ D99	2.7	2.6	2.5	9.4	T
$\alpha_1$ D94- $\beta_2$ N102	5.9	5.7	5.7	2.9	R
$\alpha_2$ Y42- $\beta_1$ D99	2.7	2.6	2.4	9.4	T
$\alpha_2$ D94- $\beta_1$ N102	5.5	5.8	5.6	2.9	R
$\alpha_1$ K40- $\beta_2$ H146	2.7	3.2	2.9	31.4	T
$\beta_2$ D94- $\beta_2$ H146	2.7	2.4	2.7	11.0	T
$\beta_2$ K144- $\beta_2$ H146	12.0	12.5	12.3	3.1	R
$\alpha_2$ K40- $\beta_1$ H146	2.5	3.1	2.4	31.4	T
$\beta_1$ D94- $\beta_1$ H146	2.8	3.8	3.1	11.0	T
$\beta_1$ K144- $\beta_1$ H146	12.4	11.7	11.7	3.1	R

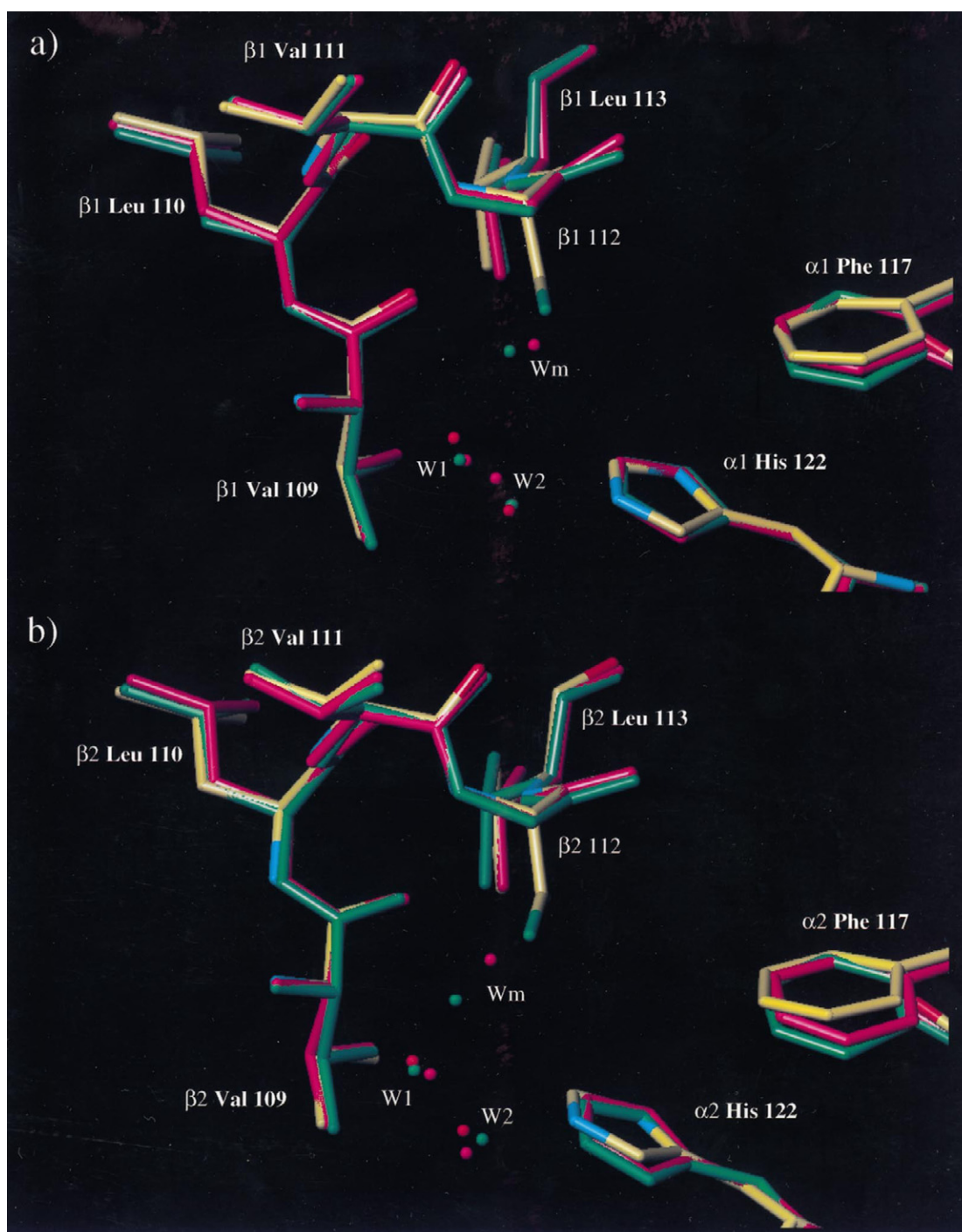


FIGURE 2 Plots of the comparison of the (a)  $\beta_1$ C112G and (b) the  $\beta_2$ C112G mutation sites in 1GBU (magenta), 1GBV (green) with natural deoxyhemoglobin, and 2HHD (Fronticelli et al., 1994a) (colored by atom type). The conserved water molecules are labeled W1 and W2, and water molecules that replace the cysteine side chain are labeled Wm.

festation of conformational changes by filling the void left by the removal of the cysteine side chain. Because of the conformational and functional similarities with natural HbA,  $\beta$ C112G is taken as reference recombinant hemoglobin for evaluating the functional effects of the single  $\beta$ 93Cys $\rightarrow$ Ala and of the double  $\beta$ 93 Cys $\rightarrow$ Ala +  $\beta$ 112Cys $\rightarrow$ Gly amino acid substitutions.

The functional characteristics of  $\beta$ C93A and  $\beta$ (C93A+C112G) are indistinguishable, consistent with the absence of conformational or functional modifications caused by the  $\beta$ 112Cys $\rightarrow$ Gly substitution. In the presence of 100 mM Cl, the replacement  $\beta$ 93 Cys $\rightarrow$ Ala at the  $\alpha_1\beta_2$  interface affects the functional properties of hemoglobin and the alkaline Bohr effect practically ends at pH 7.4 (Fig. 5). As a result, the



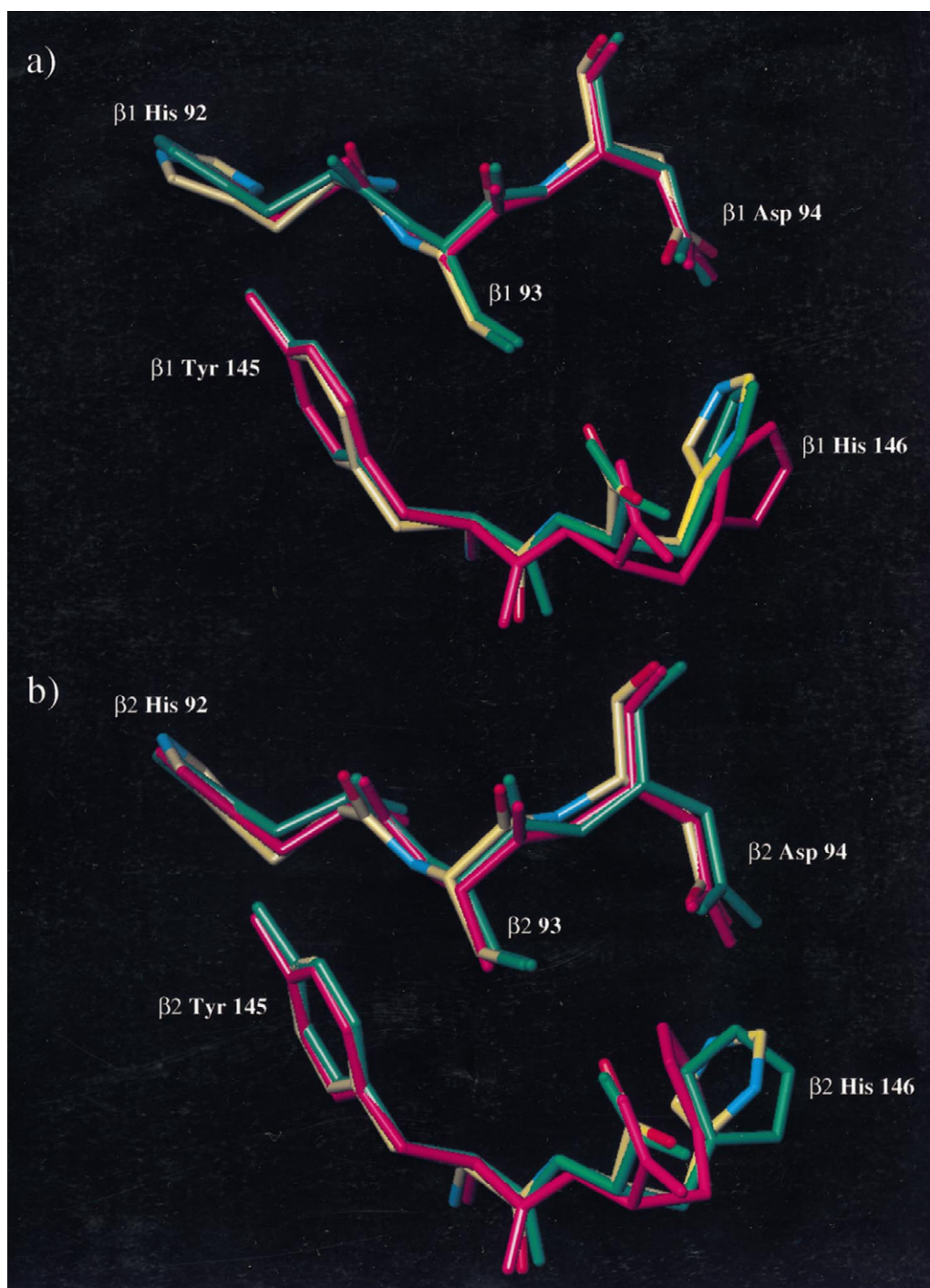


FIGURE 3 Plots of the comparison of (a) the  $\beta_1$ C93A and (b) the  $\beta_2$ C93A mutation sites in 1GBU (magenta) with 1GBV (green) and natural deoxyhemoglobin, 2HHD (colored by atom type).

protons binding capacity of the  $\beta 93$  mutants, is modified. The maximum of the curve and thus the  $pK_m$  of the Bohr groups activity is shifted by 0.4 units of pH, from 7.6 to 8.0. The maximum number of protons released upon oxygenation is decreased about 22% from 0.63/heme to 0.49/heme. The free energy of Bohr proton binding is decreased 0.5 kcal/heme from 1.8 to 1.3 kcal/heme. We attribute the origin of this functional effect to the increased conformational freedom of  $\beta 146$ His.

Crystallographic analysis indicates that upon the  $\beta 93$ Cys $\rightarrow$ Ala substitution the distance between  $\beta 146$ His-COO $^-$  and  $\alpha 40$ Lys is increased from 2.8 to 3.1 Å, weakening this salt bridge (Table 3), and that  $\beta 146$ His assumes positions that do not allow the formation of the salt bridge with  $\beta 94$ Asp (Fig. 3 and Table 3). This is functionally very relevant as  $\beta 146$ His is believed to contribute to the alkaline Bohr effect when by interacting with  $\beta 94$ Asp in T-state hemoglobin,

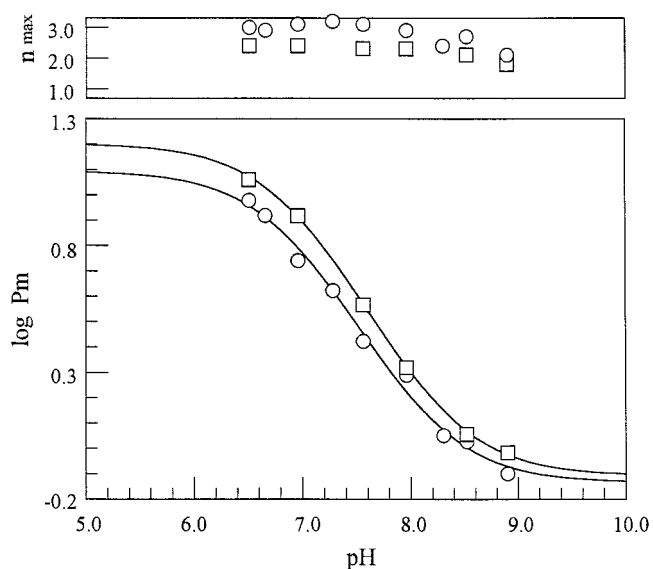


FIGURE 4 An overlay of the Bohr effect of HbA (○) and  $\beta$ C112G (□). The symbols represent the experimental data points. Solid lines are drawn using a nonlinear least squares analysis (Eq. 2 in the text). The oxygen equilibrium measurements were done in 50 mM MES/HEPES/TAPS + 100 mM  $\text{Cl}^-$  at 25°C.

forms a strong ionic interaction that increases its  $pK_a$  (Perutz et al., 1980). The decreased binding capacity and the shift in the pH of maximum proton release from 7.6 to 8.0 observed for the  $\beta$ 93 mutants in the presence of  $\text{Cl}^-$  (Fig. 7, Table 4) suggests the decreased contribution of a Bohr effect group with a  $pK_a$  somewhat lower than 7.6. This is consistent with the  $pK_a$  of 7.0 and 8.0 calculated by NMR measurements for  $\beta$ 146His in oxy and deoxy hemoglobin, respectively (Kilmartin et al.,

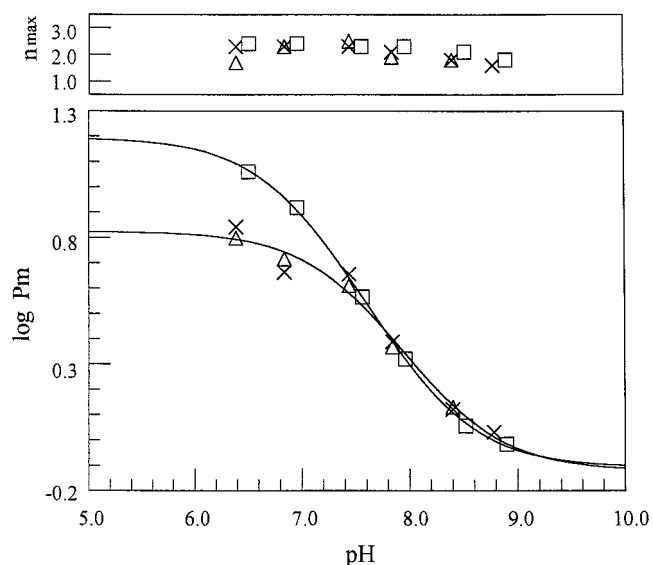


FIGURE 5 An overlay of the Bohr effect of  $\beta$ C112G (□),  $\beta$ C93A (△), and  $\beta$ (C93A+C112G) (×). The symbols represent the experimental data points. Solid lines are drawn using a nonlinear least squares analysis (Eq. 2 in the text). The oxygen equilibrium measurements were done in 50 mM MES/HEPES/TAPS + 100 mM  $\text{Cl}^-$  at 25°C.

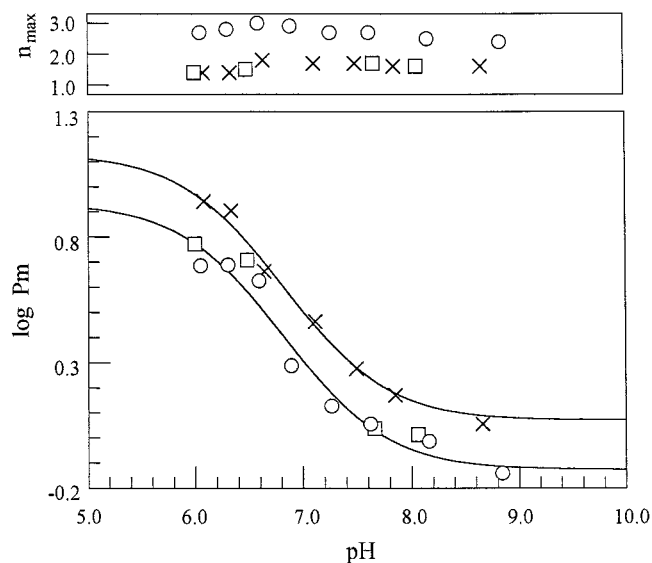


FIGURE 6 An overlay of the Bohr effect in the absence of NaCl for HbA (○),  $\beta$ C112G (□), and  $\beta$ (C93A+C112G) (×). The symbols represent the experimental data points. Solid lines are drawn using a nonlinear least squares analysis (Eq. 2 in the text). The oxygen equilibrium measurements were done in 50 mM MES/HEPES/TAPS at 25°C.

1973). In contrast, when  $\text{Cl}^-$  are absent from the solvent, the  $\beta$ 93Cys→Ala mutants have the same binding capacity and Bohr effect of  $\beta$ C112G and of HbA. (Fig. 6, Table 4). It is reasonable to propose that in  $\beta$ C93A and  $\beta$ (C93A+ $\beta$ C112G) in which in T-state  $\beta$ 146His is more mobile, the  $\text{Cl}^-$  in the solution shields the positive charge of  $\beta$ 146His, hindering its interaction with  $\beta$ 94Asp and thus altering its contribution to the Bohr effect. The possibility of an interplay between  $\beta$ 146His- $\beta$ 94Asp salt bridge and the  $\text{Cl}^-$  in the solution is supported by  $^{35}\text{Cl}^-$  NMR measurements indicating binding of  $\text{Cl}^-$  at  $\beta$ 146His in deoxy HbA (Chiancone et al., 1975), and by the low energy value of the  $\beta$ 146His- $\beta$ 94Asp salt bridge (1 kcal/mol) (Louie et al., 1988), which suggests the presence of competing interactions. In this regard we want to stress that the modification of the free energy of proton binding measured for the  $\beta$ 93 mutants is of 0.5 kcal/heme or 2.0 kcal/tetramer (Table 4). This value matches the free energy of 2.0 kcal/tetramer required for the formation of two  $\beta$ 146His- $\beta$ 94Asp salt bridges, supporting the proposal that the modified  $\beta$ 146His-

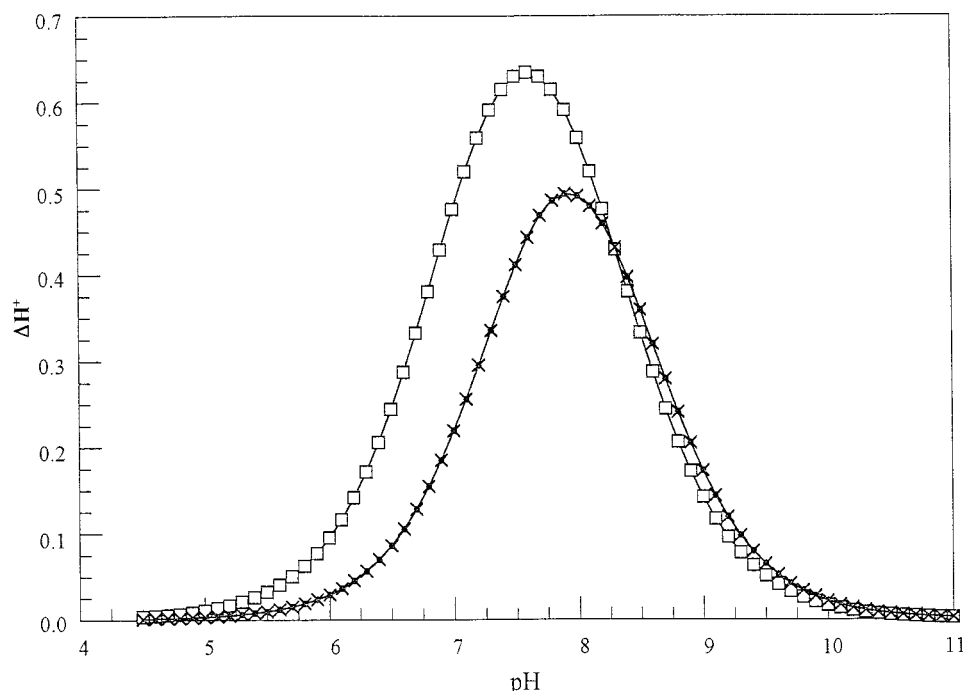
**TABLE 4** Thermodynamic parameters in the absence and in the presence of 100 mM  $\text{Cl}^-$ , derived for HbA,  $\beta$ C112G,  $\beta$ C93A, and  $\beta$ (C93A+C112G)

Protein	NaCl (mM)	$\Delta H_{\text{max}}^+$ /heme	$pK_m$	$\Delta G$ (kcal/heme)
HbA	0	0.54	7.0	1.4
$\beta$ C112G	0	0.54	7.0	1.4
$\beta$ C93A $\beta$ (C93A+C112G)	0	0.54	7.0	1.4
HbA	100	0.62	7.5	1.7
$\beta$ C112G	100	0.63	7.6	1.8
$\beta$ C93A $\beta$ (C93A+C112G)	100	0.49	8.0	1.3

Measurements were done in 50 mM MOPS/HEPES/TAPS buffer at 25°C.



FIGURE 7 Bohr protons binding capacity of  $\beta$ C112G ( $\square$ ),  $\beta$ (C93A+C112G) ( $\times$ ) in the presence of 100 mM  $\text{Cl}^-$ . These curves were drawn using Eq. 3.



$\beta$ 94Asp interaction seen by x-ray crystallography is responsible for the observed effect.

All of the recombinant hemoglobins have a decreased cooperativity, this is especially evident when  $\text{Cl}^-$  are absent from the solvent. This has also been observed with recombinant hemoglobins obtained with other expression systems (Nagai et al., 1985; Hernan and Sligar, 1995) but not for *Escherichia coli* expressed, soluble recombinant hemoglobins that have been through an oxi-reduction cycle (Shen et al., 1993), or for soluble hemoglobin expressed in yeast (De Llano et al., 1993). NMR measurements indicated the correct tetrameric assembly of our recombinant hemoglobins. We attributed the decreased cooperativity to phenomena occurring at the intermediates of oxygenation, (Sanna et al., 1997). The oxygen equilibrium curves obtained in the absence of  $\text{Cl}^-$  suggest that this effect is enhanced in the absence of effectors.

### $\beta$ 93Cys as a Bohr effect group

As the Bohr effect is decreased upon the removal of the  $\beta$ Cys93 sulfhydryl group, the possibility that  $\beta$ 93Cys could itself be an alkaline Bohr effect group should be addressed. A possible role of cysteine in the regulation of the Bohr effect was proposed by Riggs (1960) and is consistent with the different conformations of  $\beta$ 93Cys in the T- and R-state structures. Biochemical studies show that  $\beta$ 93Cys can be alkylated only while in the R-state (Riggs, 1961), which may be explained by an R-state thiolate group, though sulfhydryls are nucleophilic enough to interact with alkylating agents without the formation of a thiolate. Examination of the conformations and interactions of  $\beta$ 93Cys in the HbA structures solved in our laboratory, deoxy HbA

(2HHD) (Fronticelli et al., 1994b) and carboxy HbA (1AJ9) (Vásquez et al., 1998), show that in both allosteric conformations, the temperature factors of  $\beta$ 93Cys sulfhydryl groups were 10 and 28  $\text{\AA}^2$ , respectively, indicating that there was not unusual thermal motion of the side chains, thereby providing confidence in the assignment their positions. In the T-state structures,  $\beta$ 93Cys is accessible to the solvent but does not establish interactions with other polar residues in the protein, in particular, basic residues, which are at a distances of at least 8  $\text{\AA}$  away, respectively. In all the current R-state structures, carboxyhemoglobins 1AJ9 (Vasquez et al., 1998) and 2HCO (Baldwin, 1980), oxyhemoglobin, 1HHO (Shaanan, 1983), and R2 structure 1BBB (Silva et al., 1992),  $\beta$ 93Cys is less accessible to the solvent and at 6.7, 7.0, 6.5, and 6.84  $\text{\AA}$  distance, respectively, from the closest basic residue, the proximal histidine. This distance is too large for establishing interaction capable to stabilize a thiolate form of the sulfhydryl. Thus, it is unlikely that the  $\beta$ 93Cys is an intrinsic alkaline Bohr effect group.

There is the possibility that residues near  $\beta$ 93Cys may be potential alkaline Bohr effect groups through the influence of Cys93, but after examination of the available structures, only the penultimate  $\beta$ 145Tyr was identified as a candidate. The potential interaction of  $\beta$ 93Cys would be through an on-face H-bond from the sulfhydryl proton to the aromatic,  $\pi$  electron cloud of Tyr145. The distance between the sulfhydryl sulfur and the tyrosine ring is 3.8  $\text{\AA}$  in the R-state (1AJ9) and 4.3  $\text{\AA}$  in the T-state (2HHD), favoring this interaction in the R-state, but making the interaction improbable nonetheless. The  $\beta$ 145Tyr is also an unlikely alkaline Bohr effect group, because in a similar interaction between a threonine hydroxyl group and a tyrosine in glu-

tathione S-transferase, the interaction only lowered the  $pK_a$  0.7 units (Liu et al., 1993) and the  $pK_a$  of tyrosines range from about 9.5 to 10.9 (Metzler, 1977).

This study points to a role of  $\beta 93\text{Cys}$  in the modulation of oxygen affinity. In fact, it is the substitution  $\beta 93\text{Cys} \rightarrow \text{Ala}$  that triggers the conformational changes and the modification in the alkaline Bohr effect described in the presence of  $\text{Cl}^-$ . It also suggests that the interaction of  $\beta 146\text{His}$  with  $\beta 94\text{Asp}$  is sensitive to the presence of  $\text{Cl}^-$  in the solution.

We thank Dr. Walter Kisiel for the gift of Factor X and Dr. Enrico Bucci for a critical reading of the manuscript. The technical help of Wenxian Nie for the recombinant hemoglobin preparations is gratefully acknowledged.

This work was supported in part by the PHS National Institutes of Health Grant PO1-HL-48517.

## REFERENCES

- Ackers, G. K., M. L. Doyle, D. Myers, and M. A. Daugherty. 1992. Molecular code for cooperativity in hemoglobin. *Science*. 255:54–63.
- Adair GS. 1925. *J. Biol. Chem.* 63:529–545.
- Baldwin, J. M. 1980. The structure of human carbonmonoxy haemoglobin at 2.7 Å resolution. *J. Mol. Biol.* 136:103–128.
- Bernstein, F. C., T. F. Koetzle, G. J. B. Williams, E. F. Meyer Jr., M. D. Brice, J. R. Rogers, O. Kennard, T. Shimanouchi, and M. Tasumi. 1977. The protein data bank: a computer-based archival file for macromolecular structures. *J. Mol. Biol.* 112:535–547.
- Brunger, A. T. 1992. *X-PLOR, Version 3.1* Yale University Press, New Haven.
- Brünger, A. T., A. Krukowski, and J. Erickson. 1990. Slow-cooling protocols for crystallographic refinement by simulated annealing. *Acta Crystallogr.* A46:585–593.
- Chiancone, E., J. E. Nørre, S. Forsen, J. Bonaventura, M. Brunori, E. Antonini, and J. Wyman. 1975. Identification of chloride-binding sites in hemoglobin by nuclear-magnetic-resonance quadrupole-relaxation studies of hemoglobin digests. *Eur. J. Biochem.* 5:385–390.
- De Llano, J. J., O. Schneewind, G. Stetler, and J. M. Manning. 1993. Recombinant human sickle hemoglobin expressed in yeast. *Proc. Natl. Acad. Sci. USA*. 90:918–922.
- Di Cera, E., S. J. Gill, and J. Wyman. 1988. Binding capacity: cooperativity and buffering in biopolymers. *Proc. Natl. Acad. Sci. USA*. 85:449–452.
- Dolman, D., and S. J. Gill. 1978. Membrane-covered thin-layer optical cell for gas-reaction studies of hemoglobin. *Anal. Biochem.* 87:127–134.
- Engh, R. A., and R. Huber. 1991. Accurate bond and angle parameters for X-ray protein structure refinement. *Acta Cryst.* A47:392–400.
- Fronticelli, C., M. Gattoni, A.-L. Lu, S. W. Brinigar, J. L. Bucci, and E. Chiancone. 1994a. The dimer-tetramer equilibrium of recombinant hemoglobins. *Biophys. Chem.* 51:53–57.
- Fronticelli, C., J. K. O'Donnell, and W. S. Brinigar. 1991. Recombinant human hemoglobin: expression and refolding of beta-globin from *Escherichia coli*. *J. Prot. Chem.* 10:495–501.
- Fronticelli, C., I. Pechik, W. S. Brinigar, L. Kowalczyk, and G. L. Gilliland. 1994b. Chloride ion independence of the Bohr effect in a mutant human hemoglobin beta (V1M+H2deleted). *J. Biol. Chem.* 269:23965–23969.
- Furey, W., B. C. Wang, and M. Sax. 1982. Crystallographic computing on an array processor. *J. Appl. Crystallogr.* 15:160–166.
- Hendrickson, W. 1985. Crystallographic Computing: Data Collection, Structure Determination, Proteins, and Databases. G. Sheldrick, C. Kruger, and R. Godard, editors. Clarendon Press, Oxford, UK. 306–311.
- Hendrickson, W., and J. Konnert. 1980. Computing in Crystallography. R. Diamond, S. Ramaseshan, and K. Venkatesan, editors. Indian Academy of Sciences, Bangalore, India. 1301–1323.
- Hernan, R. A., and S. G. Sligar. 1995. Tetrameric hemoglobin expressed in *Escherichia coli*. *J. Biol. Chem.* 270:26257–26264.
- Howard, A. J., G. L. Gilliland, B. C. Finzel, T. L. Poulos, D. H. Ohlendorf, and F. R. Salemme. 1987. The use of an imaging proportional counter in macromolecular crystallography. *J. Appl. Crystallogr.* 20:383–387.
- Jia, L., C. Bonaventura, J. Bonaventura, and J. S. Stamler. 1996. S-nitrosohaemoglobin: a dynamic activity of blood involved in vascular control. *Nature*. 380:221–226.
- Jones, T. A. 1978. A graphics model building and refinement system for macromolecules. *J. Appl. Crystallogr.* 11:268–272.
- Jones, T. A., J.-Y. Zou, S. W. Cowan, and M. Kjeldgaard. 1991. Improved methods for building protein models in electron density maps and the location of errors in these models. *J. Appl. Crystallogr.* 11:268–272.
- Kilmartin, J. V., J. J. Breen, J. C. K. Roberts, and C. Ho. 1973. Direct measurement of the  $pK$  values of an alkaline Bohr group in human hemoglobin. *Proc. Natl. Acad. Sci. USA*. 70:1246–1249.
- Kilmartin, J. V., J. H. Fogg, and M. F. Perutz. 1980. Role of C-terminal histidine in the alkaline Bohr effect of human hemoglobin. *Biochemistry*. 19:3189–3193.
- Liu, S., X. Ji, G. L. Gilliland, W. J. Stevens, and R. N. Armstrong. 1993. Second-sphere electrostatic effects in the active site of glutathione S-transferase: observation of an on-face hydrogen bond between the side chain of threonine 13 and the  $\pi$ -cloud of tyrosine 6 and its influence on catalysis. *J. Am. Chem. Soc.* 115:7910–7911.
- Louie, G., T. Thao, J. J. Englander, and S. W. Englander. 1988. Allosteric energy at the hemoglobin beta chain C terminus studied by hydrogen exchange. *J. Mol. Biol.* 201:755–764.
- Luisi, B. F., and K. Nagai. 1986. Crystallographic analysis of mutant human haemoglobins made in *Escherichia coli*. *Nature*. 320:552–556.
- Metzler, D. E. 1977. *Biochemistry: The Chemical Reactions of Living Cells*, Academic Press, New York.
- Nagai, K., M. F. Perutz, and C. Poyart. 1985. Oxygen binding properties of human mutant hemoglobins synthesized in *E. coli*. *Proc. Natl. Acad. Sci. USA*. 82:7252–7255.
- Perutz, M. F. 1968. Preparation of haemoglobin Crystals. *J. Crystal Growth*. 2:54–56.
- Perutz, M. F. 1989. Mechanisms of cooperativity and allosteric regulation in proteins. *Q. Rev. Biophys.* 22:139–236.
- Perutz, M. F., J. V. Kilmartin, K. Nishikura, J. H. Fogg, P. J. G. Butler, and H. S. Rollemma. 1980. Identification of residues contributing to the Bohr effect of human haemoglobin. *J. Mol. Biol.* 138:649–668.
- Riggs, A. 1960. The nature and significance of the Bohr effect in mammalian hemoglobins. *J. General Physiol.* 39:585–605.
- Riggs, A. 1961. The binding of N-ethylmaleimide by human hemoglobin and its effect upon the oxygen equilibrium. *J. Biol. Chem.* 236:1948–1954.
- Sanna, M. T., A. Razynska, M. Karavitis, A. P. Koley, F. K. Friedman, I. M. Russu, W. S. Brinigar, and C. Fronticelli. 1997. Assembly of human hemoglobin. *J. Biol. Chem.* 272:3478–3486.
- Shaanan, B. 1983. Structure of human oxyhaemoglobin at 2.1 Å resolution. *J. Mol. Biol.* 171:31–59.
- Shen, T., N. T. Ho, V. Simplicaneau, M. Zou, B. N. Green, M. F. Tam, and C. Ho. 1993. Production of unmodified human adult hemoglobin in *E. coli*. *Proc. Natl. Acad. Sci. USA*. 90:8108–8112.
- Silva, M. M., P. H. Rogers, and A. Arnone. 1992. A third quaternary structure of human hemoglobin A at 1.7-Å resolution. *J. Biol. Chem.* 267:17248–17256.
- Vásquez, G. B., X. Ji, C. Fronticelli, and G. L. Gilliland. 1998. Human carboxyhemoglobin at 2.2 Å resolution: structure and solvent comparisons of R-state, R2-state, and T-state hemoglobins. *Acta Crystallographica*. D54:355–366.
- Wyman, J., and S. J. Gill. 1990. *Binding and Linkage*. University Science Books, Mill Valley, CA.